SAMPE Europe Conference 2019 Nantes - France

COMPARATIVE STUDIES OF STRUCTURE-PROPERTY RELATIONSHIP BETWEEN GLASS/EPOXY AND CARBON/EPOXY 3D WOVEN COMPOSITES

M. Dahale[1*], G. Neale[1], C. McGarrigle[1], J. Kelly[1], E. Archer[1], E. Harkin-Jones[1] & A. McIlhagger[1]

[1] Engineering Research Institute, Ulster University, Shore Road, Newtownabbey, Co. Antrim, BT37 0QB, United Kingdom

* Corresponding author Monali Dahale & (m.dahale@ulster.ac.uk)

ABSTRACT

This paper investigated the effect of defined weave parameters in textiles on the mechanical properties such as tension, compression, and Izod impact energy in 3D layer-to-layer glass/epoxy and carbon/epoxy woven composites. The specimens with the superior mechanical properties in both carbon and glass 3D woven composites were then tested to determine its quasi-static crash performance with a view to the end application in the automotive industry. The 3D woven preforms, manufactured using a Jacquard loom at Ulster University, were fabricated in two different weft densities: 4 & 16 wefts/cm with a constant warp density of 12 warps/cm. It was observed that changing the fibre content in the weft direction not only increased its mechanical properties in that direction but also significantly improved its performance in the warp direction (although the fibre content remains constant in the warp direction). This was thought to be result of a combination of several factors- V_f, tow misalignment, crimp, binding points/ unit cell and size/distribution of resin rich areas. This study has helped deriving a relationship between the fundamental defined weave parameters, mechanical properties and failure mechanisms in the 3D layer-to-layer warp interlock carbon/epoxy and glass/epoxy composites.

Keywords: 3D woven composites; layer-to-layer; failure modes; composite properties; weft density; through-thickness reinforcement.

1. INTRODUCTION

With the recent successful application in the LEAP project [1] to manufacture the fan blades for Airbus-A320 neo and Boeing 737-MAX aircraft, 3D woven composites are starting to pick up traction in both aerospace and automotive industry. Increasingly more and more metals have been replaced by laminated composites due to their high strength to weight and high stiffness to weight ratios [2]. The problem with these 2D laminated or UD composites is their propensity to delaminate under the influence of out-of-plane loading. With the addition of through thickness binders in 3D woven composites, delamination failure is initiated which allows the composite to carry increasing loads well beyond first crack initiation [3][4]. Moreover, 3D weaving is gaining popularity in industry over 2D weaving due to their capability to manufacture near-net-shaped preforms reducing the manufacturing/machining cost [5]. The ability to produce complex integrated structures along with excellent through-thickness strength and toughness of 3D woven composites is tempered by lower in-plane performance in comparison to 2D woven or unidirectional composites [6]. This may be further exacerbated by process induced defects or variability. In order to obtain optimum high-performance composite structures, it is essential to have a comprehensive knowledge of the effect of 3D fibre content, architecture and manufacturing defects on the properties of composites.

Performance of 3D woven composites depends on the fibre content and the orientation of binding patterns which determine the fibre architecture [7]. There are limited studies on how the weave parameters and geometrical flaws like the misalignment, voids, resin rich areas and certain topological features of the weave architecture influence the mechanical properties and their subsequent failure mechanism[8]–[10]. In the existing literature, there has always been a comparison between three standard architectures (angle interlock, orthogonal & layer-to-layer) of 3D woven composites for different properties [11][5]. To establish a fair comparison and to develop an understanding of the relationship between the weave parameters in textiles and its mechanical properties of composite materials, different weave iterations in 3D layer-to-layer architecture were considered for this study.

This research aims to investigate the influence of weft density on the mechanical and crash performance of glass and carbon 3D woven composites. The weft density changes in 3D woven preforms can be achieved by a slight change in the manufacturing process (by changing the speed of the beat-up) instead of rethreading the entire loom which takes up to over 100 hours (varies with architecture, warp/binder density etc). Also, rethreading the entire loom can cause severe damage to the warp yarns which will knockdown the mechanical properties of the subsequent composite materials [12]. Hence in this study we have considered two weft densities (4 and 16 wefts/cm) which are the minimum and maximum achievable weft density with the current weaving set-up. The specimens with the superior mechanical performance in both carbon and glass 3D woven composites were then tested for its quasi-static crash performance with an end application in automotive industry. In depth failure mechanism analysis in both carbon and glass 3D woven composites under different loading was carried out using micro-computed tomography.

2. MATERIALS

2.1 Manufacturing of 3D woven textile preforms

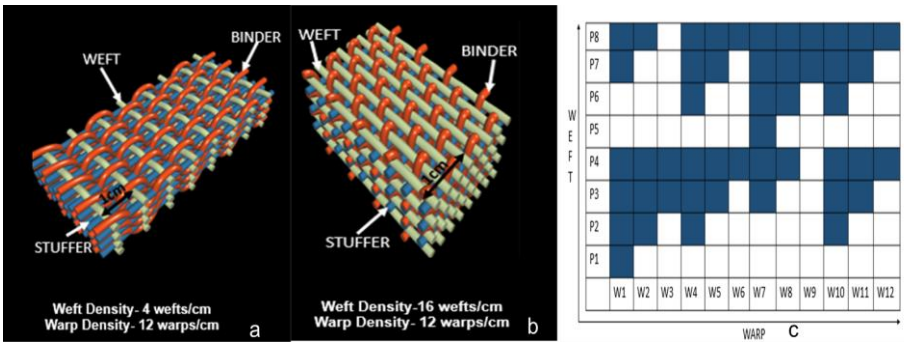

Figure 1:Diagrams representing (a & b) the 3D woven layer-to-layer architecture in two weft densities (4 & 16 wefts/cm) (d) Lift plan for Jacquard loom

3D woven layer-to-layer architectures with two different weft densities (4 and 16 wefts/cm) and a constant warp density of 12 warps/cm in both glass and carbon were developed using ScotWeave design software (Figure 1a & b). These specimens were referred to as WD1 (lower weft density) and WD2 (higher weft density) in this paper. T700S-50C-12k (800 Tex) [13] carbon fibre (1% epoxy sized) was used in the manufacture of carbon-WD1 and carbon-WD2 specimens. Hybon 2002 E-Glass (0.55% silane sized) [14] fibre was used to manufacture glass-WD1 and glass-WD2 textile preforms The lift plan (Figure 1c) developed using the ScotWeave software was used to operate the DATAWEAVE controlled Jacquard loom at Ulster University with assistance of Axis Composites Ltd.

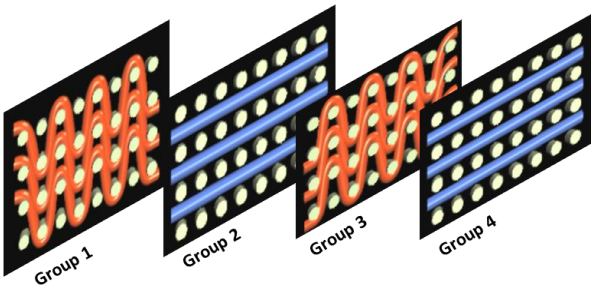

Figure 2:Group distribution of warp yarns which controlled the textile design plan

The textile design plan for this architecture was developed by dividing the unit cell structure (12 warps/cm) into four different groups (Figure 2). These four groups were as follows: Group one had three binder yarns, group two had three stuffer yarns, group three had three binder yarns and group four had three stuffer yarns. Grouping decided the placements of these yarns in the architecture by controlling the lift of the heddles in a jacquard loom. The architecture consisted of three warp layers, four weft layers and three warp binder layers which connect weft layers immediately above and below each individual binder. Binder tow paths travelled over a weft tow then downwards below the next weft layer, under the next weft tow, back above the initial weft layer. This pattern was repeated along the full length of the specimens in the warp direction. This layer-to-layer architecture was chosen due to its high conformability and only one sixth specific energy absorption (SEA) loss on transition from quasi-static to high speed dynamic loading as compared to other architectures [15]. This less energy absorption loss is beneficial for application in the automotive industry. In Figure 1 and Figure 2 , binder yarns are shown in red, stuffer yarns in blue and weft yarns are light

green in colour. The woven 3D woven preforms in WD1 and WD2 for both glass and carbon are shown in Figure 3.

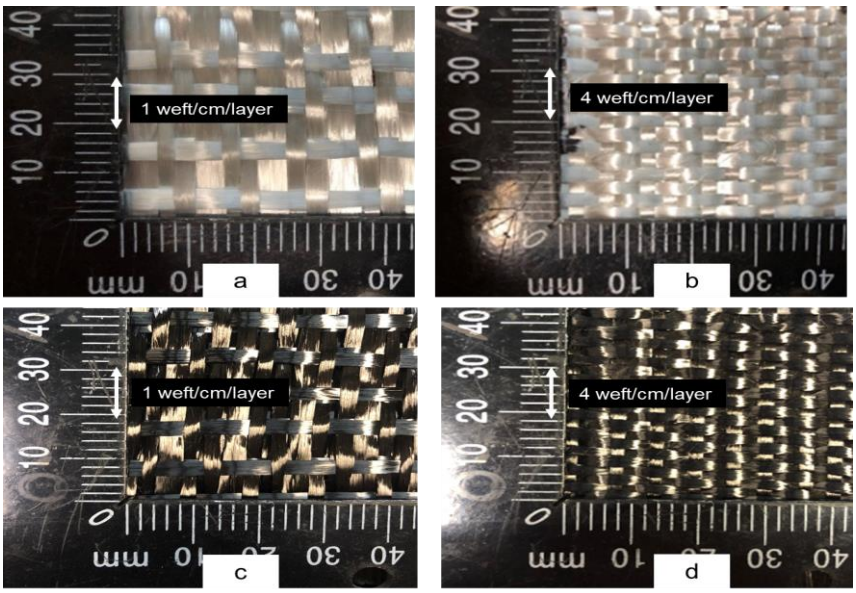

Figure 3: 3D woven textile preforms (a, b) WD1 and WD2 in glass (c,d) WD1 and WD2 in carbon

2.2 Manufacture of 3D woven composites

The WD1 and WD2 fabric preforms in glass and carbon after weaving were consolidated via Resin Transfer Molding (RTM) using a Gurit Prime 20LV epoxy resin system [16]. Prior to infusion it was degassed in a homogeniser and then injected into a preheated (30℃) RTM tool designed for the consolidation of 400x400 mm preforms. The injection pressure was maintained at 0.75 bar throughout the infusion. After injection, the part was cured at 50° C for 16 hours. For the crush specimens, the specimens with superior mechanical performance (among WD1 and WD2) were consolidated in an omega-shaped geometry (Figure 4) RTM tool of cavity size 2mm. This geometry was based on the previous work done by DLR (German Aerospace Centre) [17].

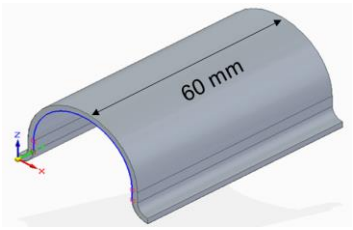

Figure 4: Omega shaped geometry for crush specimens

3. EXPERIMENTATION

3.1 3D woven preform properties

The physical properties of the textile preform like the weft density (number of transverse yarns per cm of the fabric), warp density (number of longitudinal yarns per cm of the fabric) and thickness were measured using ASTM standards [18]–[20] respectively. Crimp measurements were made in accordance with BS 2863:1984. Percentage crimp is the ratio of

the difference between the yarn length and fabric length over fabric length. It is calculated using the following equation:

$$\%Crimp = \frac{L_{yarn} - L_{fabric}}{L_{fabric}}$$

3.2 Tension

Tensile tests were performed in accordance with ASTM 3039 [21] using a Zwick Universal Testing System (UTS) with a 100kN load cell and a crosshead displacement of 2mm/min. Five specimens were tested in each direction (warp and weft). An extensometer was used to record accurate strain up to 0.6%.

3.3 Compression

Five specimens in each direction were tested for compression in accordance with a Boeing modified ASTM D695 [22] using an Instron 5500R UTS machine with 100kN load cell and anti-buckling fixture. The original test was modified by changing the specimen shape and reducing the gauge length to 4.8mm in order to avoid buckling of the test specimens.

3.4 Izod

Izod tests were performed in accordance with BS EN ISO 180:2000 [23]. Five specimens of dimensions 80mm by 10mm were manufactured oriented in both the warp and weft directions, and a 2mm deep notch was machined midway down the length.

3.5 Quasi-static crushing

Specimens with superior mechanical properties between WD1 and WD2 in both glass and carbon 3D woven composites were tested for its crash performance. Quasi-static crush testing was performed on an electromagnetic 5500R Universal Testing System (UTS) with a 100kN load cell for WD2 specimens in both carbon and glass in the warp direction. Five specimens were crushed between two steel compression platens with an initial crosshead displacement of 2mm/min for the first 15mm of displacement. The speed of crushing was then increased to 20mm/min for the remainder of the crush event.

4. RESULTS & DISCUSSION

4.1 Preform & Composite properties

Table 1:Table showing the variation in preform and composite parameters between specimens

Fabric Properties									**Composite properties**		
Fabric	Wefts/cm	Warps/cm	Thickness(mm) of uncompressed preform	Yarn content (%)			%Tow Crimp in preform		Areal density (kg/m^2)	Thickness of the composite (mm)	V_f (%)
				Warp	Weft	Binder	Warp	Weft			
Glass-WD1	4	12	2.5	37.5	25	37.5	5.1	1.4	4.6	2.4	38.2
Glass-WD2	16	12	3.9	21.4	57.2	21.4	3.7	1.1	5.4	2.8	56.5
Carbon-WD1	4	12	2.6	37.5	25	37.5	5.5	1.8	2.8	2.2	32.7
Carbon-WD2	16	12	4.2	21.4	57.2	21.4	2.8	1.7	4.5	3	53.7

The preform and composite physical properties are listed in Table 1. With the increase in the weft density, the crimp in the warp and weft tow was decreased in both carbon and

glass specimens. WD2 specimens had a more compact structure as compared to WD1, this is supported by Figure 5, in which the warp yarns in the WD1 specimens were more circular which resulted in less compaction as compared to the WD2 specimens. WD1 specimens had 66.2% more resin rich areas and tow misalignment was more significant as compared to WD2 specimens (Figure 5). Due to less compact structure in WD1 specimens, there was more free space for the preform to move in the RTM tool. During the RTM process, the permeability was higher in WD1 preforms and resin infusion time was less as compared to the WD2 specimens.

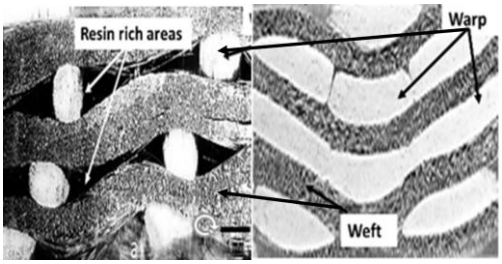

Figure 5: Micrographs of (a) WD1 composite specimens and (b) WD2 composite specimens. Note that micrographs are of carbon specimens are shown above because glass specimens are transparent

4.2 Tensile Properties

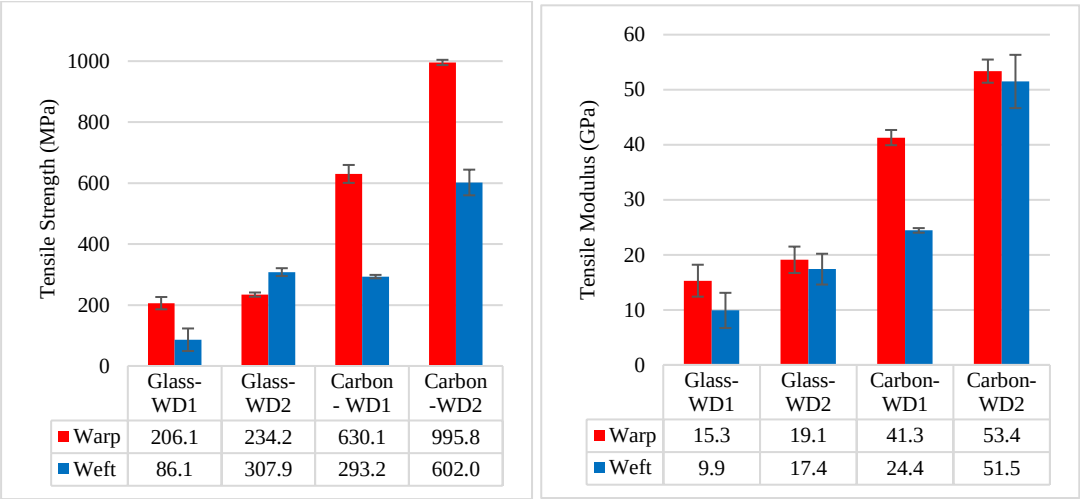

Figure 6: Tensile properties of WD1 and WD2 specimens in both glass and carbon 3D woven composites

In the weft direction specimens, there is a 257% and 75% increase in the tensile strength and modulus respectively in the glass specimens whereas 105% and 111% increase in the strength and modulus respectively in the carbon specimens with transition from WD1 to WD2 (Figure 6). This increase in both carbon and glass 3D woven composites is expected as the fibre content of the load carrying yarns is increased with weft density change from WD1 (4wefts/cm) to WD2 (16wefts/cm) specimens (Table 1). The tensile property increase is significantly higher in glass specimens going from WD1 to WD2 as compared to the carbon specimens, which is thought to be a result of a greater decrease in the crimp (27%) in glass as compared to 5% decrease in the crimp in carbon specimens on from WD1 to WD2 (Table 1).

On transition from glass to carbon 3D woven composite in higher weft density (WD2), there is an increase of 320% and 95% increase in the tensile strength in warp and

weft directions respectively. The superior performance of carbon is quite expected due to its lower density and higher in-plane properties. Eksi et al. reported an increase of 82% tensile strength on transition from glass to carbon 2D woven composite [24]. They also reported an increase of 126% tensile strength on transition from glass to carbon Unidirectional composites.

Figure 5 shows the micrographs of WD1 and WD2 specimens. WD1 specimens have more numerous and larger resin rich regions, larger than in WD2 specimens by 66.2% (Figure 5). Numerous and larger resin rich areas in WD1 specimens enables the structure to fail at lower load which results in lower tensile strength. Similar type of failure is observed in both carbon and glass 3D woven composites with transition from WD1 to WD2 (Figure 7.1). The resin rich areas promoted clean matrix fracture in the WD1 specimens with little resistance from weft yarns. The failure mechanism transitions (WD1 to WD2) from clear transverse matrix fracture, which is seen to be mostly uninterrupted by the weft yarns, to significant fibre pull out and fibre fracture in WD2 specimens (Figure 7.1 c and d). In WD2 specimens, the primary crack is forced to propagate through the fibres and the increased number of fibres promote crack branching into the laminate. More energy is required to break these fibres than is required to propagate through the matrix as observed in WD1.

From Figure 6, it is evident that the increase in weft density also moderately increases its performance in the warp direction in both carbon and glass 3D woven composites. There is a 14% and 25% increase in the tensile strength and modulus respectively in glass specimens and 58% and 29% increase in the strength and modulus respectively in carbon specimens with transition from WD1 to WD2. This can be partially attributed to a decrease in crimp of 38% and 96% in glass and carbon specimens respectively on transition from WD1 to WD2. The number of binding points per unit cell is highest in WD2 as compared to WD1. These stress concentrations result from resin rich regions which are associated with binding points as well as the tendency of the binders to straighten out during loading. This is accompanied by fibre-matrix debonding, which is likely to initiate at those points. Warp direction failure transitions from being predominantly fibre-matrix debonding dominated (while fibres remain intact) to being dominated by fibre pull out and fibre fracture (Figure 7.1 a and b). In the WD1 specimens, the tow straightening event is so severe that the specimens do not cleanly fracture but undergo a diagonal failure after ultimate strength is achieved (Figure 7.2).

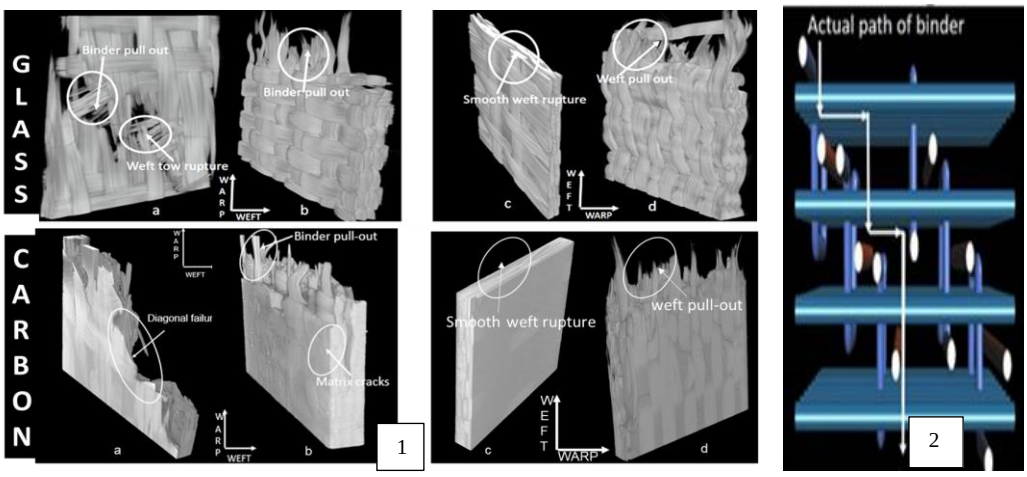

Figure 7: (1) Micro-CT images of (a, b) warp direction specimens of WD1 and WD2; (c, d) weft direction specimens of WD1 (2) Diagonal crack propagation in WD1 specimens

The diagonal crack propagation through the thickness is observed for WD1 specimen in both carbon and glass (Figure 7.1.a) This is a result of a more open architecture in the WD1 specimens which enables the binder yarns to become displaced from the original position instead of stacking neatly (Figure 5a). The crack, after initiating in the resin rich areas, follows the binder position as shown in the Figure 7.2.

4.3 Compression Properties

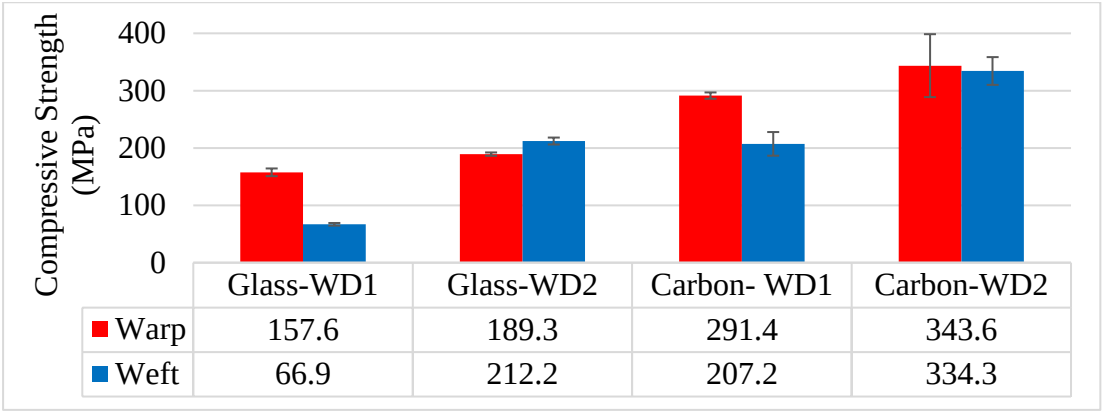

	Glass-WD1	Glass-WD2	Carbon- WD1	Carbon-WD2
Warp	157.6	189.3	291.4	343.6
Weft	66.9	212.2	207.2	334.3

Figure 8: Compressive properties of two weft density specimens in both glass and carbon.

From Figure 8 it is evident that with increasing the weft density there are significant improvements in the compressive strength in both warp and weft directions of carbon and glass specimens. In the weft direction, there is an increase of 217% and 61% compressive strength in glass and carbon specimens respectively on transition from WD1 to WD2. The increase in compressive strength in the weft direction is due to the significant increase in the percentage of fibres (4 wefts/cm to 16 wefts/cm) in that orientation.

The explanation behind improvements in the warp direction is less direct. There is an increase of 20% and 18% in strength in glass and carbon specimens respectively on transition from WD1 to WD2. This moderate increase in compressive strength is perhaps the direct result of higher geometric regularity in the composite in WD2 specimens. As per the preform design, WD1 specimens have 4 wefts/cm which equates to 1 binder turns per layer per cm. With the increase in the weft density to WD2, those same binding points are compressed into a much smaller space. Due to increased binder points in the gauge length of 4.8mm, more load is required for the specimens to fail ultimately increasing the compressive strength. The decreased unit cell in the weft direction corresponds to more binder turns in the warp direction, greater through thickness reinforcement and a greater volume of fibres oriented in the loading direction. There is an increase of 81.5% increase in the compressive strength on transition from glass to carbon in higher weft density (WD2) specimens in the warp direction. This is contrary to what was observed by Wu et al.[25]. They did not observe significant change in compressive strength on transition from glass to carbon unidirectional non crimped fabric composite of same material configuration [25].

4.4 Izod Impact Properties

The Izod impact strength results for tests are presented in Table 2. The impact strength in the weft direction is increased by 218% and 140% in glass and carbon respectively with no significant increase in the warp direction with increasing weft density from WD1 to WD2. As mentioned before, the compactness of the weave is significantly increased with weft density. The total average area and the size of resin rich regions have significantly decreased from WD1 to WD2. In the WD1 specimens, the presence of these large resin rich regions initiates

damage at lower loading. The stiffness of the material in WD2 specimens is also increased by this more compact structure which makes the material more resistant to deformation.

Table 2: Izod impact strength of two weft densities in glass and carbon 3D woven composites

Izod Impact Strength (kJ/m^2)	**Orientation**	
Specimen	Warp	Weft
Glass-WD1	183.2	67.5
Glass-WD2	210.3	214.7
Carbon-WD1	101.8	78.3
Carbon-WD2	104.8	187.9

4.5 Quasi-static crush

WD2 specimens, which showed superior mechanical properties in both glass and carbon as compared to the WD1 specimens (section 4.2, 4.3, 4.4), were characterized for its crash performance. Table 3 shows the crash performance of the WD2 specimens in both glass and carbon 3D woven layer-to-layer architecture. The specific energy absorption (SEA) of carbon specimens was 36% higher than glass specimens of the same architecture (Table 3). This is typically expected as the carbon fibre had higher strength and lower density. However, this difference is usually more apparent in 2D laminates, sometimes approaching a discrepancy of up to 70% [26]. The main observation here is that the failure modes in glass and carbon specimens differ significantly in this 3D woven architecture. Glass specimens failed via a more characteristic splaying event whereas carbon specimens failed via progressive folding. Progressive folding is uncommon in more brittle composites and is generally seen as a lower energy failure mode than splaying and other brittle fracture mechanisms. This was also supported by the results from compression testing. The carbon specimens had 82% higher compressive strength as compared to glass in WD2 architecture.

Table 3: Crush results of WD2 specimens in carbon and glass 3D woven composites

Specimen Type	**Fmax (kN)**		**Favg (kN)**		**SEA (J/g)**		**CFE (%)**	
	Avg.	Variation (%)	Avg.	Variation (%)	Avg.	Variation (%)	Avg.	Variation (%)
Glass-WD2	22.8	8.1	23.0	5.8	61.9	5.9	101.5	3.2
Carbon-WD2	28.8	6.9	27.6	0.9	84.2	2.5	96.4	6.3

5. CONCLUSIONS

The main aim of this paper is to investigate the mechanical and crash performance of 3D woven glass/epoxy and carbon/epoxy composites. The influence of weft density, distribution of resin rich areas, tow crimp and tow misalignment on the mechanical properties is also studied. The following are the observations and analysis carried out from this study: -

- A similar trend in the mechanical properties was observed with the increase in the weft density in both glass and carbon 3D woven composites. Changing the fibre content in the weft direction not only increases its mechanical properties in that direction but also significantly improves its performance in the warp direction (although the fibre content remains constant in the warp direction).
- Similar type of failure is observed under tensile and compression loading with the increase in the weft density in both carbon and glass 3D woven composites. Under

tensile loading, with increase in the weft density it transitioned from clear matrix failure to more predominantly fibre pull-out and fibre fracture. Whereas under compression loading it transitioned from inter-laminar/ brooming to micro-buckling type of failure.

- Carbon specimens showed a 36% higher specific energy absorption as compared to glass specimens. This is thought to be result of 82% higher compressive strength and 64% lower density of carbon as compared to glass specimens in WD2.

6. ACKNOWLEDGEMENTS

This work was supported by EU Horizon 2020 Marie Skłodowska-Curie Actions Innovative Training Network- ICONIC [grant agreement number: 721256]. The authors acknowledge the support from The Engineering Research Centre (ECRE) of Ulster University and Axis Composites Ltd, especially Roy Brelsford, Dr Glenda Stewart, Simon Hodge and Graeme Craig.

7. REFERENCES

[1] M. A. Jewell J, Kennedy R, "Full-scale LEAP Fan Blade-Out Rig Test Yields Outstanding Results," *Adv. LEAP Fan Endur. Test Complet.*, 2011.

[2] M. Bannister, I. Herszberg, A. Nicolaidis, F. Coman, and K. H. Leong, "The manufacture of glass/epoxy composites with multilayer woven architectures," *Compos. Part A Appl. Sci. Manuf.*, vol. 29, no. 3, pp. 293–300, 1998.

[3] J. Brandt, K. Drechslef, and F. Arendtsb, "Mechanical performance of composites based on various three-dimentional woven-fibre preforms," *Compos. Sci. Technol.*, vol. 3538, no. 95, pp. 381–386, 1996.

[4] F. Chen and J. M. Hodgkinson, "Impact behaviour of composites with different fibre architecture," *Proc. Inst. Mech. Eng. Part G J. Aerosp. Eng.*, vol. 223, no. 7, pp. 1009–1017, 2009.

[5] M. N. Saleh and C. Soutis, "Recent advancements in mechanical characterisation of 3D woven composites," *Mech. Adv. Mater. Mod. Process.*, vol. 3, 2017.

[6] M. Ansar, W. Xinwei, and Z. Chouwei, "Modeling strategies of 3D woven composites: A review," *Compos. Struct.*, vol. 93, no. 8, pp. 1947–1963, 2011.

[7] S. Dai, P. R. Cunningham, S. Marshall, and C. Silva, "Influence of fibre architecture on the tensile, compressive and flexural behaviour of 3D woven composites," *Compos. Part A Appl. Sci. Manuf.*, vol. 69, pp. 195–207, 2015.

[8] L. Tong A.P. Mouritz M. Bannister, *3D Fibre Reinforced Polymer Composites*. 2002.

[9] B. N. Cox *et al.*, "Failure mechanisms of 3D woven composites in tension, compression, and bending," *Acta Metall. Mater.*, vol. 42, no. 12, pp. 3967–3984, Dec. 1994.

[10] M. Dahale *et al.*, "Effect of weave parameters on the mechanical properties of 3D woven glass composites," *Compos. Struct.*, p. 110947, May 2019.

[11] R. Umer, H. Alhussein, J. Zhou, and W. Cantwell, *The mechanical properties of 3D woven composites*. 2016.

[12] E. Archer, S. Buchanan, A. McIlhagger, and J. Quinn, "The effect of 3D weaving and consolidation on carbon fiber tows, fabrics, and composites," *J. Reinf. Plast. Compos.*, vol. 29, no. 20, pp. 3162–3170, 2010.

[13] TORAYCA, "T700S TECHNICAL DATA SHEET CARBON," pp. 6–7.

[14] Nippon electric glass, "Direct Roving fibre glass hybon 2002," *Electric Glass Fiber America*. 2018.

[15] J. Goering and H. Bayraktar, "3D Woven Composites for Energy Absorption Applications," *SPE Automot.*, no. April, pp. 1–18, 2016.

[16] Gurit, "Prime ™ 20Lv Data Sheet." Gurit, pp. 1–6, 2015.

[17] A. Jackson, S. Dutton, A. J. Gunnion, and D. Kelly, "Investigation into laminate design of open carbon-fibre/epoxy sections by quasi-static and dynamic crushing," *Compos. Struct.*, vol. 93, no. 10, pp. 2646–2654, 2011.

[18] ASTM International, "ASTM D3775 – 03a Standard Standard Test Method for Warp End Count and Filling Pick Count of Woven Fabric 1," vol. i, pp. 1–3, 2003.

[19] ASTM INTERNATIONAL, "D3775: Standard Test Method for Warp (End) and Filling (Pick) Count of Woven Fabrics," 2018.

[20] ASTM INTERNATIONAL, "D1777: Thickness of Textile Materials." 2015.

[21] ASTM International, "ASTM D3039/D3039M Standard test method for tensile properties of polymer matrix composite materials," *Annu. B. ASTM Stand.*, pp. 1–13, 2014.

[22] ASTM INTERNATIONAL, "D695: Compressive Properties of Rigid Plastics 1." 2015.

[23] BRITISH STANDARD BS EN ISO 180:2000, "Plastics — Determination of Izod impact strength," vol. 2006, 2006.

[24] S. Ekşi and K. Genel, "Comparison of mechanical properties of unidirectional and woven carbon, glass and aramid fiber reinforced epoxy composites," *Acta Phys. Pol. A*, vol. 132, no. 3, pp. 879–882, 2017.

[25] W. Wu, Q. Wang, and W. Li, "Comparison of tensile and compressive properties of carbon/glass interlayer and intralayer hybrid composites," *Materials (Basel).*, vol. 11, no. 7, 2018.

[26] J. J. Carruthers, A. P. Kettle, and A. M. Robinson, "Energy absorption capability and crashworthiness of composite material structures: A review," *Applied Mechanics Reviews*, vol. 51, no. 10. p. 635, 1998.